

# Iterative Qubit Coupled Cluster method with involutory linear combinations of Pauli products

Robert A. Lang,<sup>1,2</sup> Ilya G. Ryabinkin,<sup>3</sup> and Artur F. Izmaylov<sup>1,2,\*</sup>

<sup>1</sup>*Department of Physical and Environmental Sciences,  
University of Toronto Scarborough, Toronto, Ontario, M1C 1A4, Canada*

<sup>2</sup>*Chemical Physics Theory Group, Department of Chemistry,  
University of Toronto, Toronto, Ontario, M5S 3H6, Canada*

<sup>3</sup>*OTI Lumionics Inc., 100 College St. #351, Toronto, Ontario M5G 1L5, Canada*

Application of current and near-term quantum hardware to the electronic structure problem is highly limited by coherence times and gate fidelities. To address these restrictions within the variational quantum eigensolver (VQE) framework, the iterative qubit coupled-cluster (iQCC) procedure [I.G. Ryabinkin *et al.*, arXiv:1906.11192] includes a portion of the ansatz not as quantum circuit elements but by unitarily transforming the Hamiltonian. iQCC has demonstrated systematic convergence towards ground state energies capable with arbitrarily shallow circuits, at the expense of exponential growth of the number of required measurements per VQE step. To reduce the growth of measurement requirements in iQCC, we present a scheme where the Hamiltonian is sequentially transformed via the unitary exponential of involutory linear combinations (ILC) of Pauli products. The ILC transformation results in quadratic growth in the number of Hamiltonian terms with the number of Pauli products included in ILC. The iQCC-ILC procedure is systematically improvable, variational, and hardware tailorable through modulation of computational cost between classical computation, number of measurements required per VQE step, and quantum circuit depths. We demonstrated that iQCC-ILC can provide chemically accurate potential energy curves for symmetric bond dissociation of H<sub>2</sub>O and LiH.

## I. INTRODUCTION

One of the most promising applications of near-term universal gate quantum computation is solving the electronic structure problem. Currently, the most feasible route to this task is through the variational quantum eigensolver (VQE),<sup>1,2</sup> which is a hybrid technique involving an iterative minimization of the electronic expectation value

$$E = \min_{\boldsymbol{\tau}} \langle \bar{0} | \hat{U}^\dagger(\boldsymbol{\tau}) \hat{H} \hat{U}(\boldsymbol{\tau}) | \bar{0} \rangle, \quad (1)$$

involving quantum and classical computers. First, a classical computer suggests a trial unitary transformation  $\hat{U}(\boldsymbol{\tau})$  that is encoded on a quantum computer as a circuit operating on the initial state of  $n_q$  qubits  $|\bar{0}\rangle \equiv |0\rangle^{\otimes n_q}$ . At the end of this circuit, one measures the expectation value of the qubit-space Hamiltonian  $\hat{H}$ , which is iso-spectral to the electronic Hamiltonian in the second quantized form. The measured electronic energy is provided to the classical computer that generates a next guess for the parameterized unitary transformation  $\hat{U}(\boldsymbol{\tau})$ . These cycles serve to minimize the energy expectation value and to approach the true electronic ground state energy. The VQE procedure has been experimentally demonstrated for small molecular systems such as LiH, BeH<sub>2</sub> and H<sub>2</sub>O.<sup>1,3-5</sup>

There are several conceptual challenges in the VQE scheme that prevent its experimental application to chemical systems beyond small molecules. First, the qubit-space electronic Hamiltonian cannot be measured entirely and requires separate measurement for its parts. The number of parts that can be measured at the same

time varies depending on the measurement technique, but it still scales at least as  $n_q^2$  for small molecules.<sup>6-12</sup> Second, choosing an efficient unitary operator form and search for the global minimum of variational parameters  $\boldsymbol{\tau}$  are exponentially hard problems that are left to heuristic processes on the classical computer. The generators of  $n_q$ -qubit unitary operations up to global phase correspond to an exponentially large Lie algebra ( $su(2^{n_q})$ ), whose elements consist of all  $n_q$ -qubit Pauli products  $\hat{P}$ ,

$$\hat{P} = \bigotimes_{j=1}^{n_q} \hat{\sigma}_j, \quad (2)$$

where  $\hat{\sigma}_j$ 's are the Pauli operators  $\{\hat{x}, \hat{y}, \hat{z}\}$  or the  $2 \times 2$  identity  $\hat{1}$  acting on the  $j^{\text{th}}$  qubit. This algebra contains  $4^{n_q} - 1$  basis generators, therefore one needs efficient heuristics to make an optimal operator choice of

$$\hat{U}(\boldsymbol{\tau}) = \prod_k e^{-i\tau_k \hat{P}_k} \quad (3)$$

compatible with hardware limited by number of reliably performed quantum circuit operations. Note that quantum computers cannot perform  $\exp(-i\tau_k \hat{P}_k)$  directly as elementary circuit operations (gates) but there are compiling schemes that present such operations as sequences of universal gates.<sup>13</sup>

Several forms for  $\hat{U}$  have been suggested recently: 1) methods based on the fermionic unitary forms restricted by the orbital excitation level and then transformed to the qubit space,<sup>1,14-16</sup> for example, unitary coupled cluster singles and doubles (UCCSD)<sup>1,5,15,17</sup>; 2) hardware based approaches, where the unitary transformation is obtained as a sequence of universal gates<sup>3,18,19</sup>;

and 3) qubit-space techniques, where  $\hat{P}_k$ 's are selected based on the sensitivity of energy to variations of their amplitudes.<sup>20–22</sup> Forms based on unitary fermionic ansatzes produce long products of unitary transformations in the qubit space (e.g. each double excitation/de-excitation unitary element is equivalent to a product of eight  $\hat{P}_k$  exponents) and thus were not used on actual quantum hardware without extra approximations. Although very frugal in the number of gates, the hardware based forms pose difficulties in efficient optimization of their parameters.<sup>23</sup> Thus, the qubit based techniques such as Qubit Coupled Cluster (QCC)<sup>20</sup> and ADAPT-VQE<sup>21,22</sup> provide some balance between the first two extremes.

To be able to reduce the gate count even further, the iterative version of QCC (iQCC) was introduced.<sup>24</sup> The main idea of iQCC is to reduce the complexity of  $\hat{U}$  implemented as a circuit by splitting it in two parts,  $\hat{U} = \hat{U}_H \hat{U}_C$ : 1)  $\hat{U}_H$  transforms the Hamiltonian,  $\hat{U}_H^\dagger \hat{H} \hat{U}_H = \hat{H}^{(d)}$  and 2)  $\hat{U}_C$  is implemented as a circuit. The transformed qubit Hamiltonian  $\hat{H}^{(d)}$  is used for evaluation of Pauli product energy gradients to construct  $\hat{U}_C$ . After optimizing  $\tau$ 's in  $\hat{U}_C$  it can be used for the Hamiltonian dressing as well, which would allow one to obtain another dressed Hamiltonian that can be used to construct next iteration of  $\hat{U}_C$ . In this scheme, a complex unitary ansatz can be achieved using arbitrarily shallow quantum circuits (and arbitrarily few simultaneously optimized parameters) by sequentially including unitary components at the operator level rather than in the state preparation. This formulation comes at the cost of exponential growth of the Hamiltonian and thus of the number of measurements required to extract the energy estimate per VQE cycle.

In this paper, to reduce the growth of the dressed Hamiltonian in iQCC, we propose a modification for the transformation procedure. The qubit Hamiltonian is transformed with unitary exponentials of  $i\tau \sum_{k=1}^N C_k \hat{P}_k$ , where the linear combination is involutory,  $(\sum_{k=1}^N C_k \hat{P}_k)^2 = \hat{1}$ . Due to this involutory property the number of terms in the transformed Hamiltonian grows only by a factor of  $O(N^2)$  per dressing with an involutory linear combination (ILC) of  $N$  Pauli terms. This scheme has the advantage of rotating the Hamiltonian to a basis whose approximate ground state may be represented with arbitrarily shallow circuits.

The rest of the paper is structured as follows. In Sec. II A we review the standard QCC ansatz and its gradient-based operator selection protocol. The general properties and conditions of the iQCC-ILC unitary ansatz are introduced in Sections II B and II C. Section II D provides explicit flow of the iQCC-ILC algorithm. In Sec. III, capabilities of the iQCC-ILC procedure are demonstrated on the dissociation potential energy curves of LiH and H<sub>2</sub>O. We provide concluding remarks and directions for future studies in Sec. IV.

## II. THEORY

### A. Qubit coupled cluster (QCC)

We start with reminding some relevant details of the QCC approach. The QCC ansatz<sup>20</sup> is built directly as a product of entangling multi-qubit rotations acting on an unentangled reference state. The reference state is taken to be the qubit-mean field (QMF) wavefunction, defined as a product of single-qubit coherent states,

$$|\mathbf{\Omega}\rangle = \bigotimes_{i=1}^{n_q} |\Omega_i\rangle, \quad (4)$$

$$|\Omega_i\rangle = \cos\left(\frac{\theta_i}{2}\right) |0\rangle + e^{i\phi_i} \sin\left(\frac{\theta_i}{2}\right) |1\rangle, \quad (5)$$

where  $\mathbf{\Omega} \equiv \{\theta_i, \phi_i\}_{i=1}^{n_q}$  are  $2n_q$  Bloch angles. The QCC wavefunction ansatz is

$$|\text{QCC}\rangle = \hat{U}_{\text{QCC}} |\mathbf{\Omega}\rangle, \quad (6)$$

$$\hat{U}_{\text{QCC}} = \prod_{i=1}^N e^{-i\tau_i \hat{T}_i/2}, \quad (7)$$

where  $\hat{T}_i$ 's are  $\hat{P}_i$ 's [Eq. (2)] containing Pauli operators for at least two qubits and are referred to as *entanglers*,  $\tau_i$ 's are corresponding variational amplitudes, and  $N$  is the number of entanglers included in the ansatz. The QCC energy is obtained by VQE optimization of the form

$$E = \min_{\mathbf{\Omega}, \boldsymbol{\tau}} \langle \mathbf{\Omega} | \hat{U}_{\text{QCC}}^\dagger(\boldsymbol{\tau}) \hat{H} \hat{U}_{\text{QCC}}(\boldsymbol{\tau}) | \mathbf{\Omega} \rangle, \quad (8)$$

where  $\boldsymbol{\tau} \equiv \{\tau_i\}_{i=1}^N$  for a set of  $\hat{T}_i$  included in  $\hat{U}_{\text{QCC}}$ . The QCC energy depends largely on  $\{\hat{T}_i\}_{i=1}^N$  entering  $\hat{U}_{\text{QCC}}$ . Individual  $\hat{T}_i$  are selected in the QCC procedure based on an energy gradient hierarchy. The energy gradient with respect to the  $\hat{T}_i$  amplitude is

$$\left. \frac{\partial E}{\partial \tau_i} \right|_{\boldsymbol{\tau}=0} = -\frac{i}{2} \langle \mathbf{\Omega}_{\min} | [\hat{H}, \hat{T}_i] | \mathbf{\Omega}_{\min} \rangle, \quad (9)$$

where  $|\mathbf{\Omega}_{\min}\rangle$  denotes the lowest-energy QMF state, i.e.  $|\mathbf{\Omega}_{\min}\rangle = \arg \min_{\mathbf{\Omega}} \langle \mathbf{\Omega} | \hat{H} | \mathbf{\Omega} \rangle$ . We denote Eq. (9) as  $\partial E / \partial \tau_i$  for brevity, where evaluation at  $\boldsymbol{\tau} = 0$  is implicitly assumed. All entanglers can be ordered by the absolute value of their energy gradient. Moreover, we found that under some mild conditions on QMF, there is no need to screen the exponential number of entanglers ( $O(4^{n_q})$ ), and one can construct directly the set of entanglers with large energy gradient magnitudes by a polynomially scaling classical algorithm.<sup>24</sup>

The condition on QMF that allows one to obtain the polynomial construction algorithm is that  $|\mathbf{\Omega}_{\min}\rangle$  has all qubits aligned along the  $z$  quantization axis, i.e.  $\theta_i \in \{0, \pi\} \forall i$ . This corresponds (up to global phase) to  $|\mathbf{\Omega}_{\min}\rangle \in \{|0\rangle, |1\rangle\}^{\otimes n_q}$ , where  $\{|0\rangle, |1\rangle\}^{\otimes n_q}$  denotes the set of  $n_q$ -qubit computational basis states. By

any fermion-to-qubit mapping,  $z$ -collinear  $|\Omega_{\min}\rangle$  corresponds to the qubit-space representation of the lowest-energy Slater determinant. In cases where  $|\Omega_{\min}\rangle$  does not have qubits aligned  $z$ -collinearly, one can instead use a “purified” collinear mean field state  $|\Phi\rangle$  for gradient evaluation Eq. (9) which has the largest overlap with  $|\Omega_{\min}\rangle$ ,

$$|\Phi\rangle = \arg \max_{|\Phi\rangle \in \{|0\rangle, |1\rangle\}^{\otimes n_q}} |\langle \Phi | \Omega_{\min} \rangle|^2. \quad (10)$$

We refer to the set of all entanglers with nonzero absolute energy gradients evaluated on  $\hat{H}$  with  $|\Phi\rangle$  as the *direct interaction set* (DIS), denoted herein as  $\mathcal{D}(\hat{H}, |\Phi\rangle)$ .

The DIS may be partitioned into  $n_p$  disjoint subsets,  $\mathcal{D} = \bigcup_{k=1}^{n_p} \mathcal{G}_k$ , where each subset  $\mathcal{G}_k$  contains  $O(2^{n_q-1})$  entanglers of identical gradient magnitude.<sup>24</sup> The number of partitions  $n_p$  for the qubit Hamiltonian scales linearly in the number of terms it contains in the fermionic representation, and hence efficient ranking of all entanglers in the DIS is accomplished by performing a gradient calculation only for a single representative entangler for each partition, thereby ranking the complete DIS of cardinality  $O(2^{n_q-1}n_p)$  with merely  $n_p$  gradient computations. Within the next section, we introduce a new unitary ansatz constructed from entanglers belonging to the DIS.

After selecting high absolute gradient  $\hat{T}_i$ 's on a classical computer and optimizing their amplitudes on a quantum or classical computer, one has a freedom to keep obtained  $\hat{U}_{\text{QCC}}$  as a circuit or use it to transform the Hamiltonian. The latter approach, iterative QCC (iQCC), leads to the exponential growth of the number of terms in the Hamiltonian with the number of  $\hat{T}_i$ 's in  $\hat{U}_{\text{QCC}}$  but reduces the circuit depth requirements. Note that dressing  $\hat{H}$  with each  $\hat{T}_i$  multiplies the number of terms in  $\hat{H}$  by only a constant factor because the Baker-Campbell-Hausdorff expansion  $\exp(i\tau_i \hat{T}_i) \hat{H} \exp(-i\tau_i \hat{T}_i)$  is finite due to the involutory property of entanglers,  $\hat{T}_i^2 = \hat{1}$ .

## B. Involutory linear combinations of entanglers

To reduce the number of terms introduced in a transformed Hamiltonian by each entangler included in  $\hat{U}_{\text{QCC}}$  we construct linear combinations of entanglers that are involutory. Using the involutory property of entanglers, one can construct an *involutory linear combination* (ILC) from set of entanglers  $\mathcal{A} = \{\hat{T}_1, \hat{T}_2, \dots\}$ ,

$$\left( \sum_{\hat{T}_i \in \mathcal{A}} \alpha_i \hat{T}_i \right)^2 = \hat{1}, \quad (11)$$

under conditions of normalization,

$$\sum_i \alpha_i^2 = 1, \quad (12)$$

and that all  $\hat{T}_i \in \mathcal{A}$  are mutually anti-commutative,

$$\{\hat{T}_i, \hat{T}_j\} = 0 \quad \forall \hat{T}_i, \hat{T}_j \in \mathcal{A}. \quad (13)$$

With the two conditions satisfied, Eq. (11) allows for the encoding of a unitary linear expansion of identity and  $|\mathcal{A}|$  mutually anti-commuting entanglers as

$$\hat{U}_{\text{ILC}} = \exp \left( -i\tau \sum_{\hat{T}_i \in \mathcal{A}} \alpha_i \hat{T}_i \right) \quad (14)$$

$$= \cos(\tau) \hat{1} - i \sin(\tau) \sum_{\hat{T}_i \in \mathcal{A}} \alpha_i \hat{T}_i. \quad (15)$$

In the iQCC-ILC procedure, unitary ILC components Eq. (14) are constructed by generating an anti-commuting subset of the DIS, and hence Eq. (15) features a linear expansion of high gradient entanglers enabling efficient energy lowering. We describe an efficient  $O(n_q^4)$  classical algorithm for generating sets of mutually anti-commuting entanglers from the DIS in Appendix A. All entanglers within the same DIS partition  $\mathcal{G}_k$  are mutually commutative. Therefore, the apparent restriction of entanglers being mutually *anti*-commutative to enter an ILC unitary enforces all entanglers to be of non-redundant gradients by construction.

Due to the linearity of Eq. (15), one can systematically obtain the optimal ILC parameters for state  $\hat{U}_{\text{ILC}} |\Phi\rangle = \left( \cos(\tau) \hat{1} - i \sin(\tau) \sum_{\hat{T}_i \in \mathcal{A}} \alpha_i \hat{T}_i \right) |\Phi\rangle$  by a general matrix eigenproblem such as one solved in a configuration interaction (CI) procedure (further details are in Appendix B).

## C. iQCC-ILC unitary dressing

The linearity of Eq. (15) has the main advantage of encoding  $N$  high-gradient entanglers while its expansion contains  $N + 1$  terms as opposed to  $O(2^N)$  for the QCC ansatz Eq. (7). A transformation of the Hamiltonian with a unitary of form Eq. (14) gives

$$\begin{aligned} \hat{U}_{\text{ILC}}^\dagger \hat{H} \hat{U}_{\text{ILC}} &= \cos^2(\tau) \hat{H} - \frac{i}{2} \sin(2\tau) \sum_{i=1}^N \alpha_i [\hat{H}, \hat{T}_i] \\ &\quad + \sin^2(\tau) \sum_{i,j=1}^N \alpha_i \alpha_j \hat{T}_i \hat{H} \hat{T}_j. \end{aligned} \quad (16)$$

An arbitrary Pauli terms commutes with half of the elements in the  $n_q$  qubit Pauli term Lie algebra while anti-commuting with the remaining half.<sup>25</sup> Hence on average commutator  $[\hat{H}, \hat{T}_i]$  contains half the number of terms in  $\hat{H}$ , and therefore the summation over  $N$  commutators in Eq. (16) on average contributes an  $N/2$  growth factor. The double summation in the last term of Eq. (16) can

be written as

$$\sum_{i,j=1}^N \alpha_i \alpha_j \hat{T}_i \hat{H} \hat{T}_j = \sum_{i=j}^N \alpha_i^2 \hat{T}_i \hat{H} \hat{T}_i + \sum_{i>j}^N \alpha_i \alpha_j (\hat{T}_i \hat{H} \hat{T}_j + \hat{T}_j \hat{H} \hat{T}_i), \quad (17)$$

where the diagonal summation does not introduce any new terms in  $\hat{H}$ . This is a consequence of the commutativity/anti-commutativity of all Pauli terms and the involutory property of  $\hat{T}_i$ 's.  $\hat{T}_i \hat{H} \hat{T}_j$  and  $\hat{T}_j \hat{H} \hat{T}_i$  can be seen to generate the same Pauli terms up to sign differences, and hence the last summation introduces an  $N(N-1)/2$  growth factor at worst. The total growth factor  $G$  for dressing with an  $N$ -entangler ILC unitary can be estimated as

$$G = 1 + N/2 + N(N-1)/2 = N^2/2 + 1. \quad (18)$$

#### D. iQCC-ILC procedure

The explicit QCC-ILC procedure with  $D$  dressing steps using ILC unitaries of at most  $N$  entanglers and final  $M$ -entangler QCC optimization is outlined below. The current iteration of the dressing procedure is denoted by  $k \geq 1$ .

1. Generate mutually anti-commuting subset  $\mathcal{A} \subset \mathcal{D}(\hat{H}^{(k)}, |\Phi^{(k)}\rangle)$  with  $|\mathcal{A}| \leq N$  using techniques outlined in Appendix A.

2. Obtain the optimal  $N$  free parameters for  $\hat{U}_{\text{ILC}} = \exp(-i\tau \sum_{\hat{T}_i \in \mathcal{A}} \alpha_i \hat{T}_i)$  for fixed mean-field reference  $|\Phi^{(k)}\rangle$  using techniques outlined in Appendix B. To account for relaxation between  $\hat{U}_{\text{ILC}}$  and the mean-field state, perform VQE optimization over the  $N$  free ILC parameters and the  $2n_q$  mean-field Bloch angles,

$$E_{\text{ILC}}^{(k)} = \min_{\Omega, \tau, \alpha} \langle \Omega | \hat{U}_{\text{ILC}}^\dagger(\tau, \alpha) \hat{H}^{(k)} \hat{U}_{\text{ILC}}(\tau, \alpha) | \Omega \rangle, \quad (19)$$

with initial guesses as the optimal coefficients obtained in Step 3 and  $|\Phi^{(k)}\rangle$  respectively.<sup>26</sup>  $\hat{U}_{\text{ILC}}$  is implemented in Eq.(19) using circuit-implementable product form Eq.(C1) further described in Appendix C. As an alternative, the relaxation step may be efficiently accomplished by classical optimization outlined in Appendix B.

3. Unitarily transform the qubit Hamiltonian as  $\hat{H}^{(k+1)} = \hat{U}_{\text{ILC}}^\dagger(\tau, \alpha) \hat{H}^{(k)} \hat{U}_{\text{ILC}}(\tau, \alpha)$  using the optimal (relaxed) ILC parameters from Step 2.

4. From optimized (relaxed)  $|\Omega\rangle$  of Step 4, obtain purified mean-field  $|\Phi^{(k+1)}\rangle$  as defined in Eq. (10), which is then used with newly transformed Hamiltonian  $\hat{H}^{(k+1)}$  for generation of updated DIS  $\mathcal{D}(\hat{H}^{(k+1)}, |\Phi^{(k+1)}\rangle)$ .

5. Let  $k = k + 1$ . If  $k < D$ , repeat steps 1-4. Otherwise, continue to step 6.

6. Select  $M$  entanglers with highest non-redundant gradient magnitudes from the final DIS,  $\{\hat{T}_i\}_{i=1}^M \subset \mathcal{D}(\hat{H}^{(D)}, |\Phi^{(D)}\rangle)$ , and perform VQE QCC energy optimization with the final unitarily transformed Hamiltonian  $\hat{H}^{(D)}$  over the  $M$  entangler amplitudes  $\tau$  and  $2n_q$  qubit Bloch angles  $\Omega$ ,

$$E = \min_{\Omega, \tau} \langle \Omega | \hat{U}_{\text{QCC}}^\dagger(\tau) \hat{H}^{(D)} \hat{U}_{\text{QCC}}(\tau) | \Omega \rangle. \quad (20)$$

We denote a iQCC-ILC procedure with  $D$  unitary transformation steps via unitary ILC components of at most  $N$  entanglers each and final QCC optimization including  $M$  entanglers as iQCC-ILC( $D, N, M$ ). As mentioned in Appendix A, the cardinality of any anti-commuting subset  $\mathcal{A} \subset \mathcal{D}$  is generally upper bound by  $2n_q - 1$ , and hence the largest ILC unitary one can construct at a single step generally includes  $N \leq 2n_q - 1$  entanglers.<sup>27</sup> It then follows that the maximum number of simultaneously optimized VQE parameters during the relaxation procedure of Step 4 is upper bound by  $O(n_q)$ , and the maximum circuit depths are upper bound by  $O(n_q)$  singly exponentiated Pauli words. An  $l$ -local exponentiated Pauli term requires  $O(l)$  controlled operations for implementation,<sup>13</sup> and hence the VQE optimization of Step 4 features maximum controlled operation counts upper bound by  $O(n_q^2)$ . In general, a iQCC-ILC( $D, N, M$ ) procedure features optimization of  $O(N+n_q)$  free parameters and  $O(Nn_q)$  controlled circuit operations during the relaxation VQE procedure (Step 4), and optimization of  $O(M+n_q)$  free parameters and  $O(Mn_q)$  controlled circuit operations for the final QCC VQE procedure (Step 6).

As an alternative to performing the relaxation procedure of Step 2 on a quantum computer, one can efficiently perform relaxed optimization completely on a classical computer using a procedure analogous to the multiconfigurational self-consistent field (MCSCF) method. Within this framework, relaxation can be iteratively accomplished by solving the ILC eigenproblem with static mean-field, followed by accounting for single-qubit relaxation by optimization of Bloch angles with fixed ILC parameters. We elaborate on this procedure in Appendix B.

The number of terms in the final transformed Hamiltonian  $\hat{H}^{(D)}$  will be  $O(N^{2D})$  times larger than the initial Hamiltonian  $\hat{H}^{(1)}$ , revealing the main advantage of the ILC unitary transformation when compared to a  $O(1.5^{ND})$  growth factor if Hamiltonian transformations were performed with standard QCC unitaries of Eq. (7). To avoid exponential blowup in number of measurements required per VQE cycle in Step 2 and 6, as well as in gradient calculations required in construction of updated DISs in Step 4, one wishes to obtain the energetically-optimal unitarily transformed Hamiltonian with small  $D$ , i.e. by maximizing  $N$ . Generally  $N \leq 2n_q - 1$  (see Appendix A), and thus  $N \approx 2n_q - 1$  is the optimal choice.

The number of transformations  $D$  in the QCC-ILC( $D, N, M$ ) algorithm may be set *a priori* by considering the worst-case estimate on the number of terms in  $\hat{H}^{(D)}$  by taking  $D$  powers of the growth factor Eq.(18). Alternatively,  $D$  may be determined *a posteriori* by convergence of  $E_{\text{ILC}}^{(k)}$  or gradient magnitudes for  $\mathcal{D}(\hat{H}^{(k)}, |\Phi^{(k)}\rangle)$ . For instance, if the difference between  $E_{\text{ILC}}^{(k)}$  and  $E_{\text{ILC}}^{(k-1)}$  falls below a given convergence threshold, or the maximum gradient magnitude for  $\mathcal{D}(\hat{H}^{(k)}, |\Phi^{(k)}\rangle)$  is below a cutoff, then  $D = k$ .

### III. NUMERICAL RESULTS

To assess the capability of the iQCC-ILC method, we perform classical simulation of the iQCC-ILC algorithm, including VQE energy estimations, to produce the potential energy surfaces (PESs) for dissociation of LiH and symmetric dissociation of H<sub>2</sub>O in the STO-3G and 6-31G basis sets respectively. Active space fermionic Hamiltonians for the LiH and H<sub>2</sub>O systems were generated and transformed to their qubit space representations by parity and Bravyi-Kitaev transformations respectively. Following qubit tapering procedures, the resulting LiH and H<sub>2</sub>O Hamiltonians act on 4- and 6-qubit spaces respectively. All details on the system Hamiltonians can be seen in Table 1 of Ref 24. Reported energy errors are with respect to the full CI (FCI) energies obtained through exact diagonalization.

A iQCC-ILC procedure of  $D$  dressings of at most  $N$ -entangler ILC unitaries with final  $M$ -entangler QCC optimization is denoted as iQCC-ILC( $D, N, M$ ), and a standard QCC procedure of  $M$  entanglers is denoted QCC( $M$ ). The QCC ansatz of Step 6 in the iQCC-ILC procedure is constructed from  $M$  highest gradient magnitude entanglers from unique partitions of the DIS. For all numerical results herein, such entanglers are generated by occupying all but one of the flip indices characterizing its respective DIS partition with  $\hat{x}$  operations, with the last index being occupied with a single  $\hat{y}$  operation. Entanglers entering the QCC ansatz do not contain  $\hat{z}$  operations since substitutions of  $\hat{z}$  and  $\hat{1}$  do not change first order energy contributions.<sup>24</sup> In cases where  $M$  is greater than the number of DIS partitions  $n_p$ , the remaining  $M - n_p$  entanglers are generated by permutations of  $\hat{x}$  with  $\hat{y}$  in the parent  $n_p$  entanglers.

Once  $M$  entanglers have been generated for inclusion in the QCC ansatz, an operator ordering strategy must be prescribed. Ordering the entanglers in Eq. (7) by highest to lowest gradient magnitude is an intuitively attractive strategy, however it can lead to exacerbated kinks along QCC-generated PESs when gradient magnitudes for the highest  $M$  partitions cross (i.e re-orderings in the DIS hierarchy occur), resulting in a re-ordering of the QCC ansatz occurring along the reaction coordinate. Such re-orderings along the PES were seen to result in kinks of up to a few kcal/mol. To alleviate the problem of discon-

tinuous PESs, we neglect re-evaluation of the DIS along the PES. In other words, the entire iQCC-ILC procedure described in Section IID is performed only once at a single geometry, whereas all other geometries do not feature re-selection of iQCC-ILC or QCC entanglers, only re-optimization of amplitudes and sequential dressing are performed. The geometry at which selection is performed can be chosen as where the first set of entangler gradients is highest.

#### LiH dissociation

We apply the iQCC-ILC procedure in producing LiH dissociation PESs of Figure 1a. All iQCC-ILC PESs are generated with dressings of 4-entangler ILC unitaries (optimization of 4 entangler amplitudes and 8 Bloch angles) and final 5-entangler QCC optimization (5 entangler amplitudes and 8 Bloch angles).

Selection of iQCC-ILC and QCC entanglers are performed at geometry  $R = 3.0$  Å, where correlation is sufficiently high,  $E_{\text{corr}} \approx 55$  kcal/mol. The entanglers selected during the iQCC-ILC procedure for this geometry are then applied for the complete PES. This way, energy discontinuities are alleviated by preserving the obtained DIS along the entire PES. While the QCC ansatz with 5 entanglers and no dressings is seen to be qualitatively sufficient, an error of up to 2 kcal/mol is observed in Figure 1b. A single dressing with an ILC unitary of 4 entanglers is seen to produce energy estimates within the chemical accuracy for the entire PES.

Further dressing is seen to improve the energy estimates for the majority of the curve. Sometimes, iQCC-ILC( $D, N, M$ ) gives higher energy than iQCC-ILC( $D - 1, N, M$ ), for example, the iQCC-ILC(2,4,5) error is marginally above the iQCC-ILC(1, 4, 5) error at extended bond length  $R > 4.2$  Å. We attribute this to use of entanglers selected at a single geometry for the entire PES, and hence dressing procedures far from the entangler ranking geometry may lead to local minima which acts as a worse starting point for the final fixed-size QCC optimization. Generally, the energy error is seen to lower for the majority of the curve with sequential dressings with entanglers selected at a single geometry.

With initial LiH qubit Hamiltonians of 100 terms, a single dressing produces Hamiltonians consisting of 135 terms. A second and further dressings yield a transformed Hamiltonian of 136 terms. This is the result of conserving the time-reversal symmetry of the original Hamiltonian by the ILC transformations. Time-reversal symmetry requires even number of  $\hat{y}$  operators in individual Pauli products and reality of their coefficients. The number of possible even  $\hat{y}$ -parity  $n_q$ -qubit Pauli terms is

$$\sum_{m=0}^{\lfloor \frac{n_q}{2} \rfloor} \binom{n_q}{2m} 3^{n_q-2m}, \quad (21)$$

which gives 136 for the  $n_q = 4$  case.

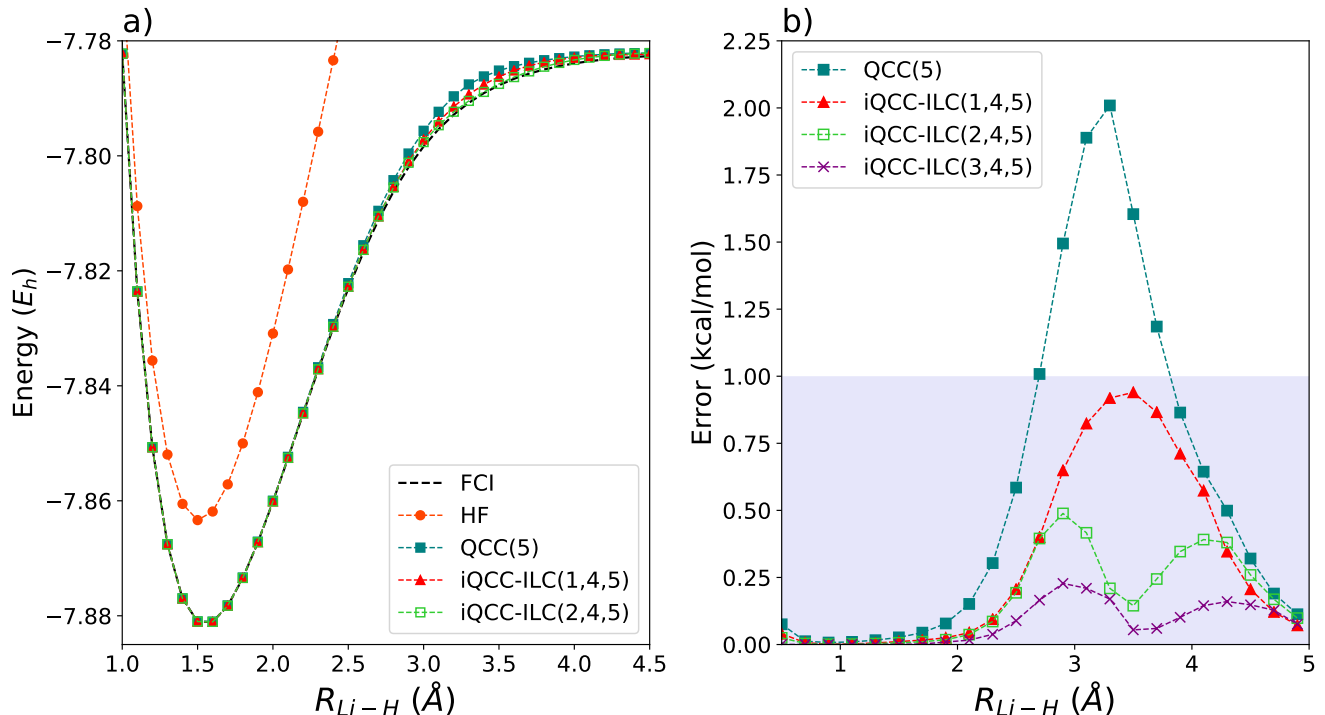


FIG. 1: a) PESs for LiH dissociation ground state for the iQCC-ILC procedure up to  $D = 3$ , and standard QCC ansatz of 5 entanglers ( $\hat{x}_1\hat{y}_3$ ,  $\hat{x}_1\hat{y}_3\hat{x}_4$ ,  $\hat{x}_1\hat{x}_2\hat{y}_3\hat{x}_4$ ,  $\hat{x}_1\hat{y}_2\hat{x}_3$ , and  $\hat{x}_1\hat{y}_2\hat{x}_3\hat{x}_4$ ) applied to undressed Hamiltonian. HF denotes the Hartree-Fock solution. b) Error comparison of the iQCC-ILC( $D, 4, 5$ ) procedure with  $1 \leq D \leq 3$  and standard QCC(5) ansatz. The shaded area denotes errors within chemical accuracy.

### H<sub>2</sub>O symmetric dissociation

We perform benchmarking of the iQCC-ILC procedure for the symmetric O-H bond dissociation of H<sub>2</sub>O. The simultaneous dissociation of both O-H bonds along the symmetric stretching of H<sub>2</sub>O is a well-known case of strong correlation and hence presents as an interesting test for the iQCC-ILC ansatz within the strongly correlated regime. We employ iQCC-ILC( $D, 8, 5$ ) schemes and consider varying numbers of transformations up to  $D = 10$  in Figure 2, to demonstrate the systematic improvability of energy estimations with constant-size quantum circuits.

To improve convergence to the singlet ground state, all calculations were performed using a spin-penalized Hamiltonian,

$$\hat{H}_s = \hat{H} + \frac{\mu}{2} \hat{S}^2, \quad (22)$$

where  $\mu$  is a positive constant ( $\mu = 0.5E_h$ ). This extra term serves as a penalty on non-singlet spin contamination during optimization. Since  $\hat{S}^2$  is a two-body operator,  $\hat{H}_s$  and  $\hat{H}$  contain the same number of terms, and hence there is no measurement overhead. All entangler selection was performed at  $R = 2.35$  Å where correlation energy is significant (185 kcal/mol).

The initial Hamiltonian  $\hat{H}_s$  for water contains 165 terms. The transformed Hamiltonian dressed with a single ILC unitary of 8 entanglers obtained in the iQCC-ILC(1, 8, 5) procedure contains 995 terms, demonstrating a  $\sim 6$  times growth factor. This is considered conservative in relation to the estimated growth factor  $G = 33$  predicted by Eq. (18). Further dressings increase the number of Hamiltonian terms to 1055, at which point the number of terms saturates. A saturation point of 1055 terms is lower than predicted by Eq. (21). However, the dressed Hamiltonians are seen to have not only even  $\hat{y}$ -parity but also even  $\hat{x}$ -parity, for which there are 1056 such Pauli products in the  $n_q = 6$  qubit Pauli product algebra. The singly-dressed iQCC-ILC(1, 8, 5) procedure is seen to qualitatively capture the PES for the symmetric dissociation, demonstrating a significant improvement over the standard QCC procedure of 5 entanglers for the spin-penalized Hamiltonian evident in Figure 2a. However, the iQCC-ILC(1, 8, 5) procedure yields an error of  $> 20$  kcal/mol for the end of the considered reaction coordinate. Systematically improved energy estimates are obtained with further dressings. The iQCC-ILC procedure with 10 transformations demonstrates microHartree accuracy for the majority of the PES, with chemical accuracy achieved for the entire considered reaction coordinate. The iQCC-ILC(2, 8, 5) procedure is already seen to

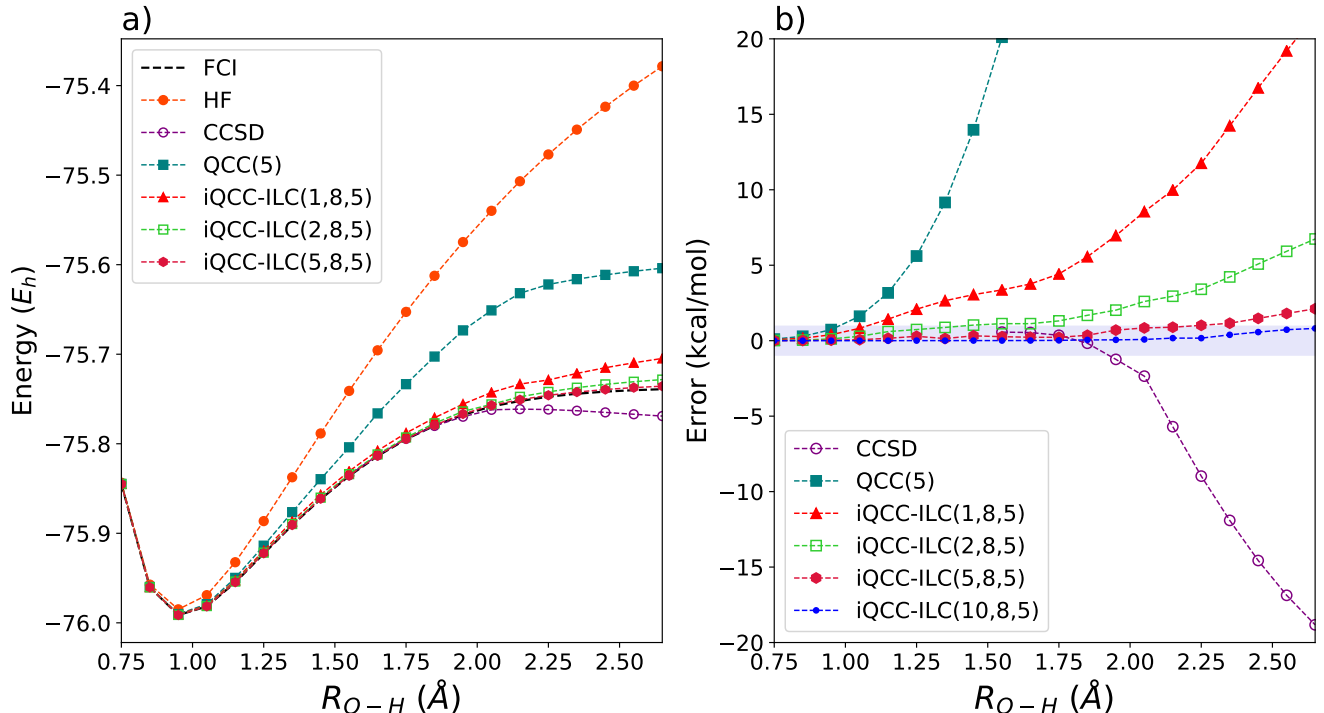


FIG. 2: a) Same as Figure 1 but for  $\text{H}_2\text{O}$  symmetric bond stretch employing spin-penalized Hamiltonian for QCC(5) (with entanglers  $\hat{x}_2\hat{y}_3\hat{x}_5\hat{x}_6$ ,  $\hat{x}_2\hat{y}_3\hat{x}_4\hat{x}_5$ ,  $\hat{x}_1\hat{y}_3$ ,  $\hat{x}_1\hat{y}_2\hat{x}_5\hat{x}_6$ , and  $\hat{x}_1\hat{y}_2\hat{x}_4\hat{x}_5$ ) and iQCC-ILC procedures. b) Error comparison of the iQCC-ILC( $D$ , 8, 5) procedures for  $1 \leq D \leq 10$ , with comparison to CCSD at extended geometries.

energetically outperform the coupled cluster with single and double excitations (CCSD) result at extended geometry (Figure 2b), the latter produces significant non-variational behaviour.

#### IV. CONCLUSION

We have introduced an iterative constructive unitary ansatz scheme that employs involutory linear combinations of Pauli products to canonically transform the qubit Hamiltonian, iQCC-ILC. The benefit of dressing the qubit Hamiltonian is to rotate to a basis where representation of the ground state may be achieved with arbitrarily low (e.g. fixed-size) circuit depth and simultaneously optimized VQE parameters at the expense of an increasing number of measurements needed to extract the energy estimate. iQCC-ILC has several advantages over iQCC. Instead of dressing with the QCC ansatz, which leads to exponential growth of the qubit Hamiltonian per dressing, dressing is performed using unitaries constructed as exponentiated ILCs, which lead to only a quadratic growth factor of the qubit Hamiltonian per dressing step. Additionally, the linearity of unitary ILCs allows for all intermediate optimizations to be efficiently performed on a classical computer, further relieving quantum resources.

The iQCC-ILC dressing is seen to aid significantly in yielding accurate energy estimates with fixed circuit depths particularly in the strongly correlated regime, exemplified in the dissociations for the LiH and  $\text{H}_2\text{O}$  systems studied. In these regions, the single-reference state  $|\Phi\rangle$  used in the undressed QCC entangler selection procedure shares little overlap with the highly correlated ground state of interest, and hence 1) considering only entanglers with first-order contribution to energy lowering may not be sufficient to recover the chemical accuracy, or 2) chemical accuracy may be recoverable with such entanglers, however only when many entanglers are included in the ansatz leading to unfavorable circuit depths. The sequential Hamiltonian transformations of the iQCC-ILC procedure have the important benefit of effectively using multi-reference state  $\hat{U}_{\text{ILC}}|\Phi\rangle$  for efficient entangler ranking by including  $\hat{U}_{\text{ILC}}$  at the operator level rather than the state. Such sequential multi-reference entangler selection protocols are advantageous for strongly correlated systems, where one may have non-negligible contribution of configurations which are connected to the initial single-reference state by higher-order contributing entanglers.

It was recently shown that projecting the qubit Hamiltonian to physical symmetry subspaces can significantly reduce the unitary ansatz depths required for VQE energy estimates at the cost of measuring a larger (pro-

jected) Hamiltonian.<sup>28</sup> It is expected that starting with a projected Hamiltonian could reduce the number of iterations required to attain chemically accurate energies within the iQCC and iQCC-ILC procedures, at the expense of a larger initial Hamiltonian. Further, incorporating recently developed strategies for optimizing the number of measurements in the VQE could be highly beneficial in mitigating the increasing number of measurements required in the iQCC-ILC scheme.<sup>7-9</sup>

## V. ACKNOWLEDGEMENTS

A.F.I acknowledges financial support from Google and the Natural Sciences and Engineering Research Council of Canada (NSERC). R.A.L acknowledges graduate student funding from NSERC.

### Appendix A: Generating mutually anti-commuting sets of entanglers

The DIS satisfies two conditions: 1) all entanglers  $\hat{T}_i \in \mathcal{D}$  must include an odd number of  $\hat{y}$  operations, denoted as having odd  $\hat{y}$ -parity, and 2) all entanglers  $\hat{T}_i \in \mathcal{D}$  with identical flip indices, defined as the qubit indices acted on by generalized “flip operations”  $\hat{f}_i \in \{\hat{x}_i, \hat{y}_i\}$ , have identical gradient magnitude.<sup>24</sup> We define the *flip index set* of a Pauli product as

$$F(\hat{P}) = \{i : \hat{f}_i \in \hat{P}\}. \quad (\text{A1})$$

The problem of generating a set of entanglers from  $\mathcal{D}$  that are suitable for ILC unitary construction can then be formulated as: given a set of  $N$  flip index sets (which characterize  $N$  distinct groupings of the DIS), generate a representative entangler for each of the flip index sets that all 1) have odd  $\hat{y}$  parity and 2) mutually anti-commute with the other  $N - 1$  representatives.

This task can be efficiently accomplished by using techniques derived from the mapping of  $n_q$  qubit Pauli terms to a  $2n_q$ -dimensional symplectic vector space over the binary field  $GF(2)$ .<sup>29</sup> By such an operator-vector space mapping, any entangler  $\hat{T}_i$  corresponds to binary vector  $\vec{T}^{(i)}$  with  $j^{\text{th}}$  and  $(n_q + j)^{\text{th}}$  components defined as

$$(\vec{T}_j^{(i)}, \vec{T}_{n_q+j}^{(i)}) = \begin{cases} (0, 1) & j^{\text{th}} \text{ qubit is } \hat{z} \\ (1, 0) & j^{\text{th}} \text{ qubit is } \hat{x} \\ (1, 1) & j^{\text{th}} \text{ qubit is } \hat{y} \\ (0, 0) & j^{\text{th}} \text{ qubit is } \hat{1} \end{cases}. \quad (\text{A2})$$

The anti-commutativity/commutativity between two Pauli terms  $\hat{T}_i$  and  $\hat{T}_j$  are then captured by the symplectic inner product,

$$\langle \vec{T}^{(i)}, \mathbf{J}\vec{T}^{(j)} \rangle = \begin{cases} 0 & \text{then } [\hat{T}_i, \hat{T}_j] = 0 \\ 1 & \text{then } \{\hat{T}_i, \hat{T}_j\} = 0 \end{cases}, \quad (\text{A3})$$

where  $\langle \cdot, \cdot \rangle$  is the regular inner product and  $\mathbf{J}$  is a symplectic metric over  $GF(2)$ ,

$$\mathbf{J} = \begin{pmatrix} \mathbf{0}_{n \times n} & \mathbf{1}_{n \times n} \\ \mathbf{1}_{n \times n} & \mathbf{0}_{n \times n} \end{pmatrix}. \quad (\text{A4})$$

Therefore the condition of all Pauli terms being mutually anti-commutative may be written as

$$\langle \vec{T}^{(i)}, \mathbf{J}\vec{T}^{(j)} \rangle = 1 \forall \vec{T}^{(i)}, \vec{T}^{(j)}. \quad (\text{A5})$$

The flip indices of a Pauli term  $\hat{T}_i$  are fully described by the first  $n_q$  components of the corresponding vector representation and treated as fixed. All  $(n_q + 1)^{\text{th}}$  to  $2n_q^{\text{th}}$  components then fully specify placements of  $\hat{1}_j$  and  $\hat{z}_j$  on non-flip indices ( $\vec{T}_j^{(i)} = 0$ ) and  $\hat{x}_j$  and  $\hat{y}_j$  on flip indices ( $\vec{T}_j^{(i)} = 1$ ) and are hence treated as variables. To ensure a Pauli term has odd  $\hat{y}$ -parity, one requires an odd number of  $(\vec{T}_j^{(i)}, \vec{T}_{n_q+j}^{(i)}) = (1, 1)$  occurrences in  $\vec{T}^{(i)}$ . All Pauli terms  $\hat{T}_i$  having odd  $\hat{y}$ -parity then satisfy

$$\langle \vec{T}^{(i)}, \mathbf{\Omega}\vec{T}^{(i)} \rangle = 1 \forall \vec{T}^{(i)}, \quad (\text{A6})$$

where

$$\mathbf{\Omega} = \begin{pmatrix} \mathbf{0}_{n \times n} & \mathbf{1}_{n \times n} \\ \mathbf{0}_{n \times n} & \mathbf{0}_{n \times n} \end{pmatrix}. \quad (\text{A7})$$

The conditions of Eqs. (A5) and (A6) yield  $N(N + 1)/2$  binary equations for which we solve for  $Nn_q$  variables. Generally, the system of equations is overdetermined when  $N > 2n_q - 1$ , which serves as a general upper bound on  $N$  for an iQCC-ILC unitary component, comparable to cardinality  $2n_q + 1$  of maximally anti-commuting sets of Pauli terms not restricted by  $\hat{y}$ -parity.<sup>25</sup> Solutions can be found by formulating conditions Eqs. (A5) and (A6) to  $N(N + 1)/2$  by  $Nn_q$  matrix  $\mathbf{A}$  and performing  $GF(2)$  Gaussian elimination for

$$\mathbf{A}\mathbf{z} = \mathbf{1}, \quad (\text{A8})$$

where  $\mathbf{1}$  is the  $N(N + 1)/2$ -dimensional vector with 1 in all components, and solutions of  $\mathbf{z}$  give the  $Nn_q$  variables fully defining the  $N$  entanglers satisfying both sets of conditions Eqs. (A5) and (A6). Finite field Gaussian elimination has  $O(m^3)$  time complexity for  $m$  variables,<sup>30</sup> hence obtaining solution to Eq.(A8) can be done in  $O(N^3n_q^3)$  time. Since  $N$  is bound to  $O(n_q)$ , the worst-case scaling of this procedure is  $O(n_q^6)$ .

There exist instances of  $\mathbf{A}$  for which  $\mathbf{1}$  is not in its image, i.e. Eq.(A8) has no solution. In cases where no solution exists, we employ greedy method of replacing the lowest gradient flip index set considered with the next-lowest gradient set until a solution can be found to the corresponding  $\mathbf{A}$ . If there exists no next-lowest gradient flip index set in the greedy process, the lowest is simply removed, and an effective  $N = N - 1$  is used.

## Appendix B: Obtaining optimal iQCC-ILC unitary parameters

The state generated by acting a given iQCC-ILC unitary component,  $\hat{U}_{\text{ILC}}$ , on the single-reference QMF state  $|\Phi\rangle$  may be written

$$\hat{U}_{\text{ILC}}|\Phi\rangle = \exp\left(-i\tau \sum_{i=1}^N \alpha_i \hat{T}_i\right)|\Phi\rangle \quad (\text{B1})$$

$$\equiv c_1|\Phi\rangle - i \sum_{j=2}^{N+1} c_j \hat{T}_j |\Phi\rangle, \quad (\text{B2})$$

where  $c_1 = \cos(\tau)$  and  $c_j = \sin(\tau)\alpha_{j-1}$ . Letting  $|\Phi_1\rangle \equiv |\Phi\rangle$ , and  $|\Phi_j\rangle \equiv \hat{T}_j|\Phi\rangle$  for  $j > 1$ , one has by construction,

$$\langle\Phi_i|\Phi_j\rangle = \delta_{ij}, \quad (\text{B3})$$

since all  $\hat{T}_j$  in the involutory combination are necessarily characterized by different flip indices and  $|\Phi\rangle$  is a computational basis state. Finding the optimal amplitudes and energy minimum can hence be done by generating Hamiltonian matrix  $\mathbf{H}$  in the set of  $N + 1$  orthogonal basis functions  $\{|\Phi_j\rangle\}_{j=1}^{N+1}$ ,

$$H_{ij} \equiv \langle\Phi_i|\hat{H}|\Phi_j\rangle, \quad (\text{B4})$$

from which the energy minimum and optimal parameters  $\{c_j\}_{j=1}^{N+1}$  can be obtained via standard orthogonal eigenproblem formulation. The imaginary phase of the summed over configurations in Eq. (B2) can be explicitly accounted for by modifying the Hamiltonian matrix by element-wise multiplication,  $\bar{\mathbf{H}} = \mathbf{M} \circ \mathbf{H}$ , where

$$\mathbf{M} = \begin{pmatrix} 1 & -\mathbf{i}_{1 \times N} \\ \mathbf{i}_{N \times 1} & \mathbf{1}_{N \times N} \end{pmatrix}. \quad (\text{B5})$$

The optimal coefficients  $\{c_i\}_{i=1}^{N+1}$  in Eq. (B2) may then be obtained by solving for the ground state solution of

$$\bar{\mathbf{H}}\mathbf{c} = E\mathbf{c}, \quad (\text{B6})$$

where  $E$  corresponds to the energy minimum for the unitary combination,

$$E = \min_{\tau, \alpha} \langle\Phi|\hat{U}_{\text{ILC}}^\dagger(\tau, \alpha)\hat{H}\hat{U}_{\text{ILC}}(\tau, \alpha)|\Phi\rangle. \quad (\text{B7})$$

Unique matrix elements of  $\mathbf{H}$  may be efficiently obtained on a classical computer due to the polynomial scaling of evaluating mean-field expectation values as trigonometric polynomial functions of the  $2n_q$  Bloch angles.<sup>31</sup> Once Eq. (B6) has been solved, iQCC-ILC component parameters  $\{\tau, \alpha_1, \dots, \alpha_N\}$  may be extracted from ground eigenvector  $\mathbf{c}$  by obtaining amplitude  $\tau$  as

$$\tau = \arccos(c_1), \quad (\text{B8})$$

which can then be used to obtain  $\{\alpha_i\}_{i=1}^N$ ,

$$\alpha_{j-1} = \frac{c_j}{\sin \tau}. \quad (\text{B9})$$

From Eq. (B9),  $\{\alpha_i\}_{i=1}^N$  are undefined when  $\tau = 0$  (modulo  $\pi$ ), however, such a scenario does not happen in practice. This is a result of all entanglers being selected from the DIS, and hence have non-zero gradient evaluated at  $\tau = 0$ , ensuring the optimized  $\tau$  amplitude will be non-zero.

## Relaxation step

The procedure described above will obtain the optimal ILC amplitudes for the initial collinear mean-field state. As an alternative to performing VQE optimization of  $2n_q + N$  parameters, simultaneous relaxation of the mean-field Bloch angles and ILC amplitudes can be accomplished on a classical computer by an MCSCF-like two step procedure: 1) solve generalized eigen-problem for subspace Hamiltonian matrix resolved in the  $N + 1$  states to obtain the current-step optimal ILC amplitudes  $\{\tau, \alpha_1, \dots, \alpha_N\}$ , and 2) dress initial Hamiltonian  $\hat{H}$  with the ILC unitary using obtained ILC amplitudes of the current step

$$\tilde{H} = \hat{U}_{\text{ILC}}^\dagger(\tau, \alpha)\hat{H}\hat{U}_{\text{ILC}}(\tau, \alpha), \quad (\text{B10})$$

then perform Bloch angle optimization with respect to  $\tilde{H}$ . The current-step optimized mean-field state is then used to update the subspace basis of Step 1. The two steps are then repeated until convergence of the energy, yielding the relaxed  $N$  ILC amplitudes and  $2n_q$  Bloch angles. Over the course of optimization, the mean-field state may violate  $z$ -collinearity, resulting in subspace basis states  $|\Phi_1\rangle \equiv |\Omega\rangle$ ,  $|\Phi_j\rangle \equiv \hat{T}_j|\Omega\rangle$ ,  $j > 1$  no longer being generally orthogonal. Step 1 must hence be accomplished by solving non-orthogonal generalization of B6,

$$\bar{\mathbf{H}}\mathbf{c} = E\bar{\mathbf{S}}\mathbf{c}, \quad (\text{B11})$$

where  $\bar{\mathbf{S}} = \mathbf{M} \circ \mathbf{S}$  and  $\mathbf{S}_{ij} = \langle\Phi_i|\Phi_j\rangle$ .

## Appendix C: Product representation of the iQCC-ILC unitary

A step in the iQCC-ILC algorithm outlined in Section (IID) can be implemented by VQE optimization of the ILC parameters, requiring implementation of  $\hat{U}_{\text{ILC}}$  as a quantum circuit. While an ILC component Eq. (14) is fundamentally implementable on a universal gate quantum computer due to unitarity, their implementation is not immediately straightforward due to the inability to decompose general exponentiated Pauli sums directly to a universal gate set. We require an exact form of Eq. (14) represented as a product of singly exponentiated Pauli terms. For  $N \equiv |\mathcal{A}|$ , a product of  $2N - 1$  exponentiated Pauli terms resembling a symmetric Trotter-Suzuki

decomposition<sup>32–34</sup> can be used to exactly represent the exponentiated linear combination,

$$\exp\left(-i\tau \sum_{i=1}^N \alpha_i \hat{T}_i\right) = \prod_{i=1}^N e^{-i\beta_i \hat{T}_i/2} \prod_{i=N}^1 e^{-i\beta_i \hat{T}_i/2}, \quad (\text{C1})$$

using the features of mutual anti-commutativity of  $\hat{T}_i \in \mathcal{A}$  and normalization of  $\{\alpha_i\}_{i=1}^N$ . Expanding all terms in symmetric product Eq. (C1) by the involutory property of individual Pauli terms, one can write the expansion of a iQCC-ILC component of  $N$  entanglers as

$$\hat{U}_{\text{ILC}} = \prod_i^N \cos(\beta_i) \hat{1} - i \sum_{i=1}^N \sin(\beta_i) \hat{T}_i \prod_{j>i}^N \cos(\beta_j). \quad (\text{C2})$$

From Eq. (C2) it is evident that  $\{\beta_i\}_{i=1}^N$  behave as hyper-spherical angles defining  $N + 1$  coordinates on the  $N$ -dimensional unit sphere. Likewise, amplitudes  $\{\tau, \alpha_1 \dots \alpha_N\}$  in Eq. (14) fully parameterize  $N + 1$  coordinates  $\{c_i\}_{i=0}^N$  on the  $N$ -dimensional unit sphere as seen in Eq. (15), where  $c_0 = \cos(\tau)$ , and  $c_i = \sin(\tau)\alpha_i$ . Therefore  $\{\beta_i\}_{i=1}^N$  are uniquely related to  $\{\tau, \alpha_1 \dots \alpha_N\}$  through the coordinate transformation

$$\beta_1 = \begin{cases} \arcsin \frac{c_1}{\sqrt{c_0^2 + c_1^2}} & c_0 \geq 0 \\ \pi - \arcsin \frac{c_1}{\sqrt{c_0^2 + c_1^2}} & c_0 < 0 \end{cases}, \quad (\text{C3})$$

$$\beta_i = \arcsin \frac{c_i}{\sqrt{\sum_{j=0}^i c_j^2}}, \quad 1 < i \leq N. \quad (\text{C4})$$

\* artur.izmaylov@utoronto.ca

- <sup>1</sup> A. Peruzzo, J. McClean, P. Shadbolt, M.-H. Yung, X.-Q. Zhou, P. J. Love, A. Aspuru-Guzik, and J. L. O'Brien, *Nat. Commun.* **5**, 4213 (2014).
- <sup>2</sup> D. Wecker, M. B. Hastings, and M. Troyer, *Phys. Rev. A* **92**, 042303 (2015).
- <sup>3</sup> A. Kandala, A. Mezzacapo, K. Temme, M. Takita, M. Brink, J. M. Chow, and J. M. Gambetta, *Nature* **549**, 242 (2017).
- <sup>4</sup> I. G. Ryabinkin, S. N. Genin, and A. F. Izmaylov, *J. Chem. Theory Comput.* **15**, 249 (2019).
- <sup>5</sup> C. Hempel, C. Maier, J. Romero, J. McClean, T. Monz, H. Shen, P. Jurcevic, B. P. Lanyon, P. Love, R. Babbush, A. Aspuru-Guzik, R. Blatt, and C. F. Roos, *Phys. Rev. X* **8**, 31022 (2018).
- <sup>6</sup> A. F. Izmaylov, T. C. Yen, and I. G. Ryabinkin, *Chem. Sci.* **10**, 3746 (2019).
- <sup>7</sup> T.-C. Yen, V. Verteletskiy, and A. F. Izmaylov, *arXiv e-prints* (2019), arXiv:1907.09386 [quant-ph].
- <sup>8</sup> A. F. Izmaylov, T.-C. Yen, R. A. Lang, and V. Verteletskiy, *Journal of Chemical Theory and Computation* **16**, 190 (2020).
- <sup>9</sup> V. Verteletskiy, T.-C. Yen, and A. F. Izmaylov, *arXiv e-prints* (2019), arXiv:1907.03358 [quant-ph].
- <sup>10</sup> A. Zhao, A. Tranter, W. M. Kirby, S. F. Ung, A. Miyake, and P. Love, *arXiv e-prints* (2019), arXiv:1908.08067 [quant-ph].
- <sup>11</sup> O. Crawford, B. van Straaten, D. Wang, T. Parks, E. Campbell, and S. Brierley, *arXiv e-prints* (2019), arXiv:1908.06942 [quant-ph].
- <sup>12</sup> W. J. Huggins, J. McClean, N. Rubin, Z. Jiang, N. Wiebe, K. B. Whaley, and R. Babbush, *arXiv e-prints* (2019), arXiv:1907.13117 [quant-ph].
- <sup>13</sup> J. T. Seeley, M. J. Richard, and P. J. Love, *J. Chem. Phys.* **137** (2012).
- <sup>14</sup> J. Lee, W. J. Huggins, M. Head-Gordon, and K. B. Whaley, *J. Chem. Theory Comput.* **15**, 311 (2019).
- <sup>15</sup> I. Sokolov, P. K. Barkoutsos, P. J. Ollitrault, D. Greenberg, J. Rice, M. Pistoia, and I. Tavernelli, *arXiv.org* (2019), arXiv:1911.10864 [quant-ph].
- <sup>16</sup> F. A. Evangelista, G. Kin-Lic Chan, and G. E. Scuseria, *arXiv* (2019), arXiv:1910.10130 [physics.chem-ph].
- <sup>17</sup> W. Mizukami, K. Mitarai, Y. O. Nakagawa, T. Yamamoto, T. Yan, and Y.-y. Ohnishi, *arXiv e-prints* (2019), arXiv:1910.11526 [cond-mat.str-el].
- <sup>18</sup> B. T. Gard, L. Zhu, G. S. Barron, N. J. Mayhall, S. E. Economou, and E. Barnes, *arXiv.org* (2019), 1904.10910v1.
- <sup>19</sup> M. Ganzhorn, D. Egger, P. Barkoutsos, P. Ollitrault, G. Salis, N. Moll, M. Roth, A. Fuhrer, P. Mueller, S. Werner, I. Tavernelli, and S. Filipp, *Phys. Rev. Applied* **11**, 044092 (2019).
- <sup>20</sup> I. G. Ryabinkin, T.-C. Yen, S. N. Genin, and A. F. Izmaylov, *J. Chem. Theory Comput.* **14**, 6317 (2018).
- <sup>21</sup> H. R. Grimsley, S. E. Economou, E. Barnes, and N. J. Mayhall, *Nat. Commun.* **10**, 3007 (2019).
- <sup>22</sup> H. L. Tang, E. Barnes, H. R. Grimsley, N. J. Mayhall, and S. E. Economou, *arXiv.org* (2019), 1911.10205v1.
- <sup>23</sup> J. R. McClean, S. Boixo, V. N. Smelyanskiy, R. Babbush, and H. Neven, *Nat. Commun.* **9**, 1 (2018).
- <sup>24</sup> I. G. Ryabinkin, R. A. Lang, S. N. Genin, and A. F. Izmaylov, *arXiv e-prints* (2019), arXiv:1906.11192 [quant-ph].
- <sup>25</sup> R. Sarkar and E. van den Berg, *arXiv e-prints* (2019), arXiv:1909.08123 [quant-ph].
- <sup>26</sup> Optionally, one can allow for a finite number of VQE optimizations using random guesses for ILC parameters and Bloch angles to reduce possibility of convergence to local minima or saddle points.
- <sup>27</sup> The cardinality of anticommuting sets of entanglers is generally bound by  $2n_q + 1$ , however the additional constraint of all entanglers having odd  $\hat{y}$ -parity reduces the bound to  $2n_q - 1$ .
- <sup>28</sup> T.-C. Yen, R. A. Lang, and A. F. Izmaylov, *J. Chem. Phys.* **151**, 164111 (2019).
- <sup>29</sup> S. Bravyi, J. M. Gambetta, A. Mezzacapo, and K. Temme, *arXiv e-prints*, arXiv:1701.08213 (2017).
- <sup>30</sup> M. Mézard and A. Montanari, *Information, Physics, and Computation*, Oxford Graduate Texts (OUP Oxford, 2009).
- <sup>31</sup> S. N. Genin, I. G. Ryabinkin, and A. F. Izmaylov, *arXiv e-prints* (2019), arXiv:1901.04715 [physics.chem-ph].
- <sup>32</sup> M. Suzuki, *J. Stat. Phys.* **43**, 883 (1986).
- <sup>33</sup> M. Suzuki, *Phys. Lett. A* **165**, 387 (1992).
- <sup>34</sup> M. Suzuki, *Phys. Lett. A* **180**, 232 (1993).